ACS APPLIED MATERIALS & INTERFACES

RESEARCH ARTICLE

www.acsami.org

Solution−Liquid−Solid Synthesis of $CuInSe_2$ Nanowires and Their Implementation in Photovoltaic Devices

Chet Steinhagen, Vahid A. Akhavan, Brian W. Goodfellow, Matthew G. Panthani, Justin T. Harris, Vincent C. Holmberg, and Brian A. Korgel*

Department of Chemical Engineering, Center for Nano- and Molecular Science and Technology, and Texas Materials Institute, The University of Texas at Austin, Austin, Texas 78712-1062

Supporting Information

ABSTRACT: $CuInSe_2$ (CIS) nanowires were synthesized by solution−liquid−solid (SLS) growth in a high boiling solvent using bismuth nanocrystals as seeds. The nanowires tended to be slightly deficient in In and exhibited either cubic or hexagonal crystal structure, depending on the synthesis conditions. The hexagonal structure, which is not observed in bulk crystals, appears to evolve from large concentrations of twin defects. The nanowires could be compressed into a free-standing fabric or paper-like material. Photovoltaic devices (PVs) were fabricated using the nanowires as the light-absorbing layer to test their viability as a solar cell material and were found to exhibit measurable PV response.

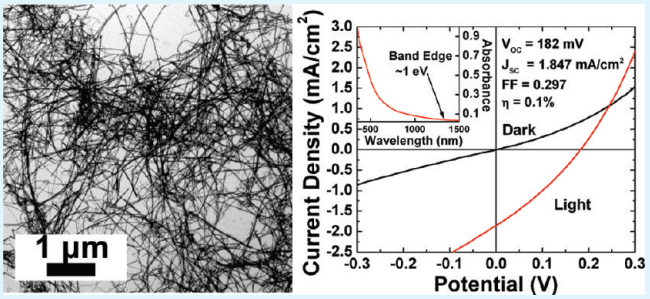

KEYWORDS: $CuInSe_2$, nanowires, photovoltaics, solar cells

INTRODUCTION

Copper indium diselenide ($CuInSe_2$; CIS) and related I−III−VI_2 compounds have been established as useful semiconductors for thin film photovoltaic devices (PVs), or solar cells, achieving high power conversion efficiencies (PCEs) and commercial use.[1] Conventional fabrication of these PVs, however, requires vapor deposition and high temperature processing, which leads to high manufacturing cost and limits the range of device architectures that can be made. Significantly lower cost could be achieved by processing the materials by inexpensive roll-to-roll printing methods with high throughput under ambient conditions. One approach to achieving this goal is to use colloidal nanocrystal inks to deposit the inorganic light-absorber layers. This approach has been demonstrated by a number of research groups,[2−9] but the PCEs are still too low for commercialization.

One of the main limitations of device efficiency with absorber layers composed of nanocrystals is the large number of interfaces or grain boundaries in the film.[7,8] Hillhouse and Agrawal[3,10] have alleviated this problem by sintering their CIS-based nanocrystal films at high temperature (~500 °C) under Se atmosphere to achieve PCE of greater than 10%. This approach, however, still relies on high temperature processing. In contrast to nanocrystals, nanowires do not have grain boundaries along their length. Nanowires can also be dispersed in solvents and deposited on substrates under ambient conditions. Therefore, using nanowires, it might be possible to improve minority carrier diffusion lengths and device efficiency in printed inorganic PVs without sintering.[11−13]

Recently, CIS nanowires have been synthesized by vapor−liquid−solid (VLS)[14−17] and solution−liquid−solid (SLS)[18] approaches. Since the SLS process yields large quantities of nanowires, we explored this approach to make CIS nanowires, applying a variation of the methods described by Wooten et al.[18] using bismuth (Bi) nanocrystals as growth seeds. We found that CIS nanowires can be produced in significant quantity with little particulate byproduct but often have large concentrations of twin defects. Under some reaction conditions, the nanowires form with wurtzite crystal structure, a phase that does not appear in the bulk. The nanowires also tend to be deficient in In. As a test to determine if the nanowires are potentially viable as light-absorbing material for use in PV devices, nanowires were spray-deposited onto substrates and packaged into PV devices. The nanowires gave a measurable PV response, with a power conversion efficiency under AM 1.5 illumination of 0.1%. Although the actual device efficiency is relatively low, these results demonstrate that the nanowires may be viable PV material.

EXPERIMENTAL METHODS

Chemicals. All chemicals were used as received. Tetrahydrofuran (THF, anhydrous, ≥99.9%, inhibitor-free), sodium bis(trimethylsilyl)-amide (Na[$N(SiMe_3)_2$], 1.0 M in THF), bismuth chloride ($BiCl_3$, ≥98%), diphenyl ether (DPE, 99%), copper(I) acetate (97%), indium(III) acetate (99.99%), indium(III) chloride ($InCl_3$, 99.999%), elemental selenium (Se, 99.99%), trioctylphosphine (TOP, 90%), oleic acid (OA, 99%), squalane (99%), and 1-hexadecylamine (HDA, 90%) were obtained from Aldrich; methanol (MeOH), toluene, and hexane were

Received: March 16, 2011
Accepted: March 31, 2011
Published: March 31, 2011

from Fisher Scientific. Polyvinylpyrrolidone−hexadecane (PVP-HDE) copolymer (Ganex V-216, MW = 7300 g/mol, product ID 72289D) was from ISP Technologies, Inc.

Bismuth Nanocrystal Synthesis. Tris[bis(trimethylsilyl)amino] bismuth ($Bi[N(SiMe_3)_2]_3$) was synthesized by previously reported methods and dissolved in THF to make a 1 M solution.[19] Five grams of Ganex V216 and 15 g of diphenyl ether were combined in a 100 mL three-neck flask. The flask was attached to a Schlenk line, placed under vacuum, heated to 70 °C, and allowed to degas for 1.5 h while stirring. In parallel, 0.5 mL of $Bi[N(SiMe_3)_2]_3$/THF was mixed with 2.0 mL of 1 M $NaN(SiMe_3)_2$ in THF and placed into a syringe. After the Ganex V216 and diphenyl ether solution was degassed, the flask was refilled with N_2 and the temperature was increased to 180 °C. At 180 °C, the Bi precursor solution was quickly injected into the hot solution and reacted for 30 min. After 30 min, the mixture was cooled to 60 °C and 15 mL of room-temperature toluene was added.

Bi nanocrystals were isolated by centrifuging the reaction product for 3 min at 5000 rpm. The supernatant was collected, and the precipitate was discarded. Thirty milliliters of MeOH was added to the supernatant and centrifuged for 5 min at 10 000 rpm. The supernatant was discarded. The precipitate was dispersed in 10 mL of toluene. This process was repeated several times, and the final precipitate was dispersed and stored in toluene at a concentration of 5 mg/mL. The Bi nanocrystals were spherical with an average diameter of 12.7 ± 0.9 nm (see Supporting Information).

$CuInSe_2$ Nanowire Synthesis. A 1 M stock solution of Se in TOP (TOP/Se) was made by dissolving 1.58 g of Se powder in 20 mL of TOP. This solution was made in a glovebox under an inert atmosphere, stirred overnight to ensure that the Se was completely dissolved, and stored in the same glovebox.

Copper acetate (30.6 mg, 0.25 mmol), 70.3 mg of indium acetate (0.25 mmol), 0.25 mL of OA, and 4 mL of TOP were combined in a 25 mL three-neck flask. The flask was attached to a Schlenk line and degassed while heating to 100 °C. After reaching 100 °C, the solution was held under vacuum for 15 min and stirred vigorously. The flask was then filled with N_2 and cooled to room temperature under N_2 flow.

In a separate 50 mL three-neck flask, 8.5 mL of TOP was added, attached to the Schlenk line, and degassed under vacuum at room temperature for 5 min. The TOP was heated to 360 °C under N_2 flow (this describes a typical reaction; other temperature, solvent, and precursor combinations were tried as described in the paper).

The Cu and In precursor solution was then combined with 0.5 mL of the 1 M TOP/Se stock solution and placed in a syringe. To initiate the reaction, 0.25 mL of a 5 mg/mL solution of Bi nanocrystals in toluene was swiftly injected into the hot TOP, followed immediately by the Cu, In, and Se precursor solution. The reaction mixture immediately turned from a light yellow color to dark brown with some black precipitate forming. The reaction proceeded for 5 min followed by removal of the heating mantle, allowing the products to cool to ∼50 °C.

Ten milliliters of toluene was then injected into the flask, after which this solution was removed from the Schlenk line. To separate and clean the products, this mixture was centrifuged at 4000 rpm for 5 min. The supernatant was discarded, and the precipitate was redispersed in 30 mL of toluene. This cleaning procedure was repeated three times, and the final product was redispersed in ∼10 mL of toluene. Tens of milligrams of CIS nanowires are obtained from typical reactions.

Nanowire Photovoltaic Device Fabrication. PV devices were fabricated on soda lime glass substrates with a layered Au/CIS NW/CdS/ZnO/indium tin oxide (ITO) structure. Gold back contacts were deposited by thermal evaporation (Lesker). CIS nanowires were deposited by spray coating from a toluene dispersion. The CdS buffer layer was deposited by chemical-bath deposition. Substrates were placed on a hot plate at 90 °C, and then, 0.9 mL of an aqueous solution of 1.25 mL of 0.015 M $CdSO_4$ (Aldrich, 99.999%), 2.2 mL of 1.5 M thiourea (Fluka, 99%), and 2.8 mL of 14.28 M NH_4OH (Fisher Scientific, Certified ACS) were placed on the substrate. After 2 min, the substrates were rinsed with deionized water and dried in air. ZnO/ITO top contacts were deposited by radio frequency (rf) sputtering from ZnO (99.9%, Lesker) and ITO (99.99% 90:10 In_2O_3/SnO_2, Lesker) targets. The active region of the device was 8 mm^2.

Fabrication of CIS Nanowire Fabric. CIS nanowire fabric was made by vacuum-filtration. A dispersion of CIS nanowires was passed through a porous alumina filter (Whatman Anodisc 13, 0.2 μm pores). The fabric on the filter was then dried in air for ∼1 h and removed from the filter with tweezers. The thickness of the fabric could be adjusted by adding different amounts of dispersion before drying.

Materials Characterization. The nanowires were characterized by transmission electron microscopy (TEM), scanning electron microscopy (SEM), and X-ray diffraction analysis (XRD). TEM images were obtained on 200 mesh carbon-coated Ni grids (Electron Microscopy Sciences) using a FEI Tecnai Spirit BioTwin operated at 80 kV. High-resolution TEM images and energy-dispersive X-ray spectroscopy (EDS) data were obtained using a JEOL 2010F transmission electron microscope operated at 200 kV and equipped with an Oxford INCA EDS detector. SEM images were obtained using gold-coated soda lime glass substrates with a Zeiss Supra 40 VP scanning electron microscope operated at 1−10 keV. XRD data were acquired on a Bruker-Nonius D8 Advance powder diffractometer using Cu Kα radiation (λ = 1.54 Å) with samples on quartz substrates, scanning at 12 deg/min in 0.02° increments.

PV devices were tested on a Karl Suss probe station and an Agilent 4156C parameter analyzer. J-V data and power conversion efficiencies were obtained using a Keithley 2400 General Purpose Sourcemeter and a Xenon Lamp Solar Simulator (Newport) with an AM 1.5 filter. Incident photon conversion efficiency (IPCE) data were collected using a lock-in amplifier (Stanford Research Systems, model SR830), a monochromator (Newport Cornerstone 260 1/4M), and Si and Ge photodiodes calibrated by the manufacturer (Hamamatsu).

RESULTS AND DISCUSSION

CIS Nanowire Synthesis. Figure 1 shows TEM and SEM images of CIS nanowires synthesized by Bi nanocrystal-seeded SLS growth. Reactions were carried out by dispersing Bi nanocrystals in toluene and adding them to a flask of hot TOP at 360 °C in an oxygen-free atmosphere, followed immediately by the injection of a reactant solution of indium acetate, copper acetate, and selenium in trioctylphosphine (TOP). After 5 min of reaction time, the nanowires have reached several micrometers in length, with an average diameter of around 20 nm. Most nanowires had Bi particles at their tips, as in Figure 1b, and reactions carried out without Bi nanocrystals did not yield nanowires (See Supporting Information), confirming that Bi nanocrystals were indeed seeding nanowire formation.

The nanowires are crystalline, as confirmed by TEM and XRD. Figure 2 shows a typical XRD pattern for a nanowire sample. The XRD of this nanowire sample is consistent with tetragonal (chalcopyrite) CIS; however, elemental analysis by energy-dispersive X-ray spectroscopy (EDS) showed that the nanowires were deficient in In, with an average composition of $Cu_{1.0}In_{0.6}Se_{2.0}$. The CIS nanowires made by this SLS process always tended to be In deficient. Furthermore, only slightly modified reaction conditions led to CIS nanowires with the cubic phase. The cubic phase is structurally similar to chalcopyrite but lacks positional cation order. XRD of chalcopyrite CIS exhibits additional reflections compared to sphalerite, like the (101) and (211) planes for example. The intensity of these two peaks is characteristically low, making it difficult in practice to distinguish between the two phases; however, nanowires could clearly be made with chalcopyrite phase, as confirmed by the

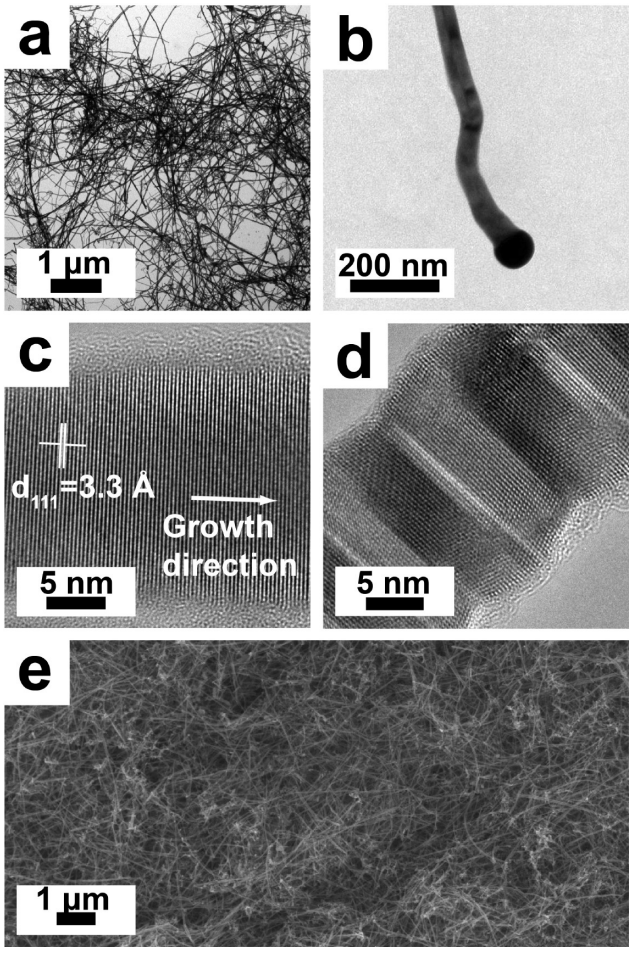

Figure 1. (a–d) TEM and (e) SEM images of $CuInSe_2$ (CIS) nanowires.

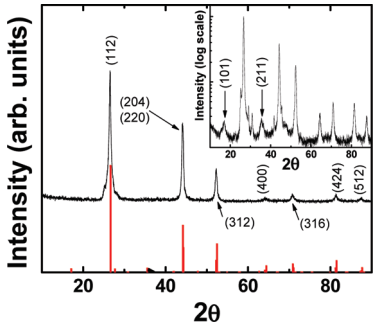

Figure 2. XRD of CIS nanowires synthesized with $InCl_3$ in TOP or indium acetate in squalane (inset, plotted on a logarithmic scale to elucidate the (101) and (211) peaks). The red reference pattern corresponds to chalcopyrite CIS (JCPDS no. 97-006-8928).

XRD pattern in the inset in Figure 2 from CIS nanowires synthesized at 400 °C in squalane (rather than TOP), but most reaction conditions led to nanowires with sphalerite structure.

Twinning and Wurtzite Crystal Structure. The predominant growth direction of the nanowires was always perpendicular to the chalcopyrite (112) or sphalerite (111) lattice planes. Figure 1c shows a high resolution TEM image of a nanowire with lattice spacing of 0.33 nm, which corresponds to either the chalcopyrite (112) or cubic (111) *d*-spacing. Virtually all of the CIS nanowires made by the SLS

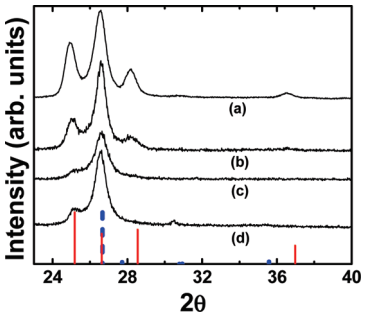

Figure 3. XRD patterns of CIS nanowires synthesized at 400 °C (a), 360 °C (b), 270 °C (c), and 360 °C with HDA (d). The dashed blue reference pattern corresponds to chalcopyrite CIS (JCPDS no. 97-006-8928), and the red reference pattern was simulated with CaRIne Crystallography 3.1 software using space group $P6_3mc$ and lattice parameters a = 4.08 Å and c = 6.69 Å.

process also exhibited significant twinning. Figure 1d shows an example of a nanowire with lamellar twinning and its characteristic zigzag surface structure.[20] In some cases, the twinning was so extensive that it led to nanowires with wurtzite structure. Figure 3 shows XRD patterns of nanowires that have extra diffraction peaks at 2θ of ~25°, 28°, and 37°. In a previous report of CIS nanowire synthesis, a Cu_3Se_2 impurity was observed;[18] however, Cu_3Se_2 does not give rise to a peak at 37°, ruling out the possibility that Cu_3Se_2 was present in the nanowires synthesized here. We found that the diffraction pattern indexes well to wurtzite $CuInSe_2$ (Figure 3). This phase does not occur in bulk CIS but has been observed in nanocrystals.[21,22] The formation of nanowires with wurtzite structure is also well-known for III–V compounds, like GaAs, InAs, and even Si, that have cubic structure in the bulk.[23–25]

Subtle changes in the reaction conditions had a significant effect on the quality, crystal phase, and morphology of the nanowire product. Figure 4 shows TEM images of nanowire product obtained under different reaction conditions. The amount of wurtzite phase was generally less at lower reaction temperature and when HDA was added (Figure 3). CIS nanowires made with $InCl_3$ instead of indium acetate had cubic structure (Figure 2), but the nanowires exhibited a rough, sawtooth morphology, as the TEM in Figure 4c shows. Nanowires grown at 400 °C in squalane were composed of chalcopyrite CIS, but the reaction product contained a significant amount of particulate byproduct (Figure 4a). Figure 4b shows that the nanowire morphology was greatly improved when TOP was added to the solvent (for a 50/50 mixture of TOP and squalane), but a small quantity of agglomerates still remained. The highest quality nanowires were synthesized at 360 °C with HDA added to the reaction. These nanowires had smooth surfaces (Figure 4d), little particulate byproduct, and mostly the cubic phase (Figure 3, pattern d).

CIS Nanowire "Fabric". One aspect of the SLS growth of CIS nanowires is its compatibility with industrial scaleup and capability of producing commercially relevant quantities of material. The relatively large quantity of CIS nanowires produced by this reaction allows for the fabrication of a nonwoven semiconductor "fabric". This fabric is made by a simple vacuum filtration of a CIS nanowire dispersion. Figure 5 shows SEM images of the CIS nanowire paper. This semiconductor nanowire fabric represents an entirely new class of materials and opens the possibility of creating novel, flexible and lightweight inorganic solar cells.

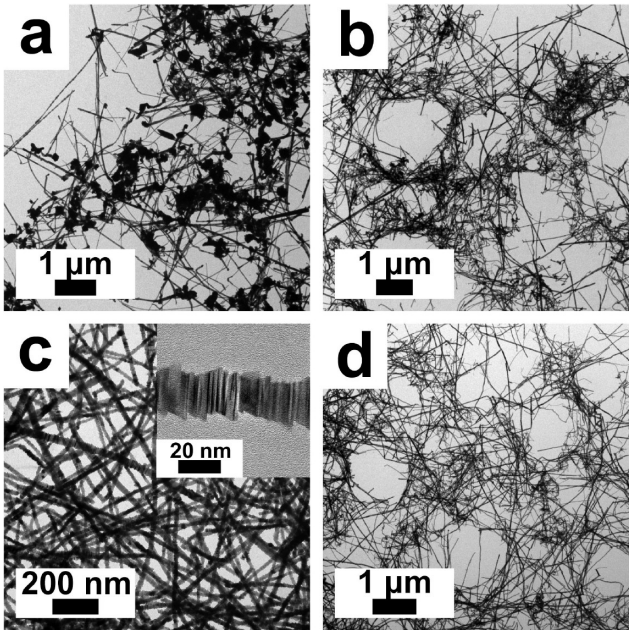

Figure 4. Low resolution transmission electron microscopy (LRTEM) and high resolution transmission electron microscopy (HRTEM; c, inset) images of CIS nanowires synthesized under various reaction conditions: (a) in squalane, (b) in a 50/50 vol % mixture of squalane and TOP, (c) in TOP with $InCl_3$ as the In source (instead of $In(acac)_3$), and (d) in TOP with added HDA.

Experiments are currently being conducted to assess the viability of the use of this nanowire fabric as the active layer in photovoltaic devices.

CIS Nanowire PV Performance. The nanowires were tested as the light-absorbing material in a solar cell to determine if the nanowire material is viable for that application. The PV test devices were fabricated with CIS nanowires in a layered architecture of Au/CIS NWs/CdS/ZnO/indium tin oxide (ITO). The CIS nanowires were deposited by spray coating a toluene dispersion. Figure 6 shows the PV response of a typical test device: the open-circuit voltage (V_{OC}) is 182 mV, the short-circuit current density (J_{SC}) is 1.847 mA/cm^2, the fill factor (FF) is 0.297, and the PCE (η) is 0.1% under AM 1.5 illumination.

The incident photon conversion efficiency (IPCE) of the CIS nanowire devices was also measured. Figure 7 shows the IPCE of a typical CIS nanowire device. Although the IPCE of the device is low, there is photocurrent generation at wavelengths longer than 510 nm (the band-edge wavelength of CdS), proving that the CIS nanowires are the photoactive material in the device.

The PV response of the nanowire devices provides a proof-of-principle that these materials can perform in solar cells. The relatively poor performance of the devices is due to a variety of factors related to the device itself. The low values of V_{OC} and FF are due in part to low shunt resistance caused by voids in the nanowire film. Although the nanowire films were relatively uniform (Figure 1e shows an SEM image of a nanowire film), there were voids in the layer, which lead to a low shunt resistance under light. The nanowire orientation is also not optimized. Nanowires lay parallel to the electrode interface with a random orientation as a tangled mat. Charge separation would be better with nanowires spanning directly between the two electrodes. For these purposes, the nanowires made here are probably too long. Furthermore, defects in the nanowires could be contributing to the poor device characteristics. For example, twinning in nanowires has been shown to be detrimental to carrier transport,[27] and vacancies related to In deficiency in the nanowires could also inhibit device performance. Ideally, phase−pure, twin-free, stoichiometric chalcopyrite CIS nanowires are desired. The phase purity of the nanowires depends rather sensitively on the reaction temperature and the presence of surfactants such as HDA, while the morphology was affected by reaction temperature, solvent, and the choice of precursor and requires more optimization.

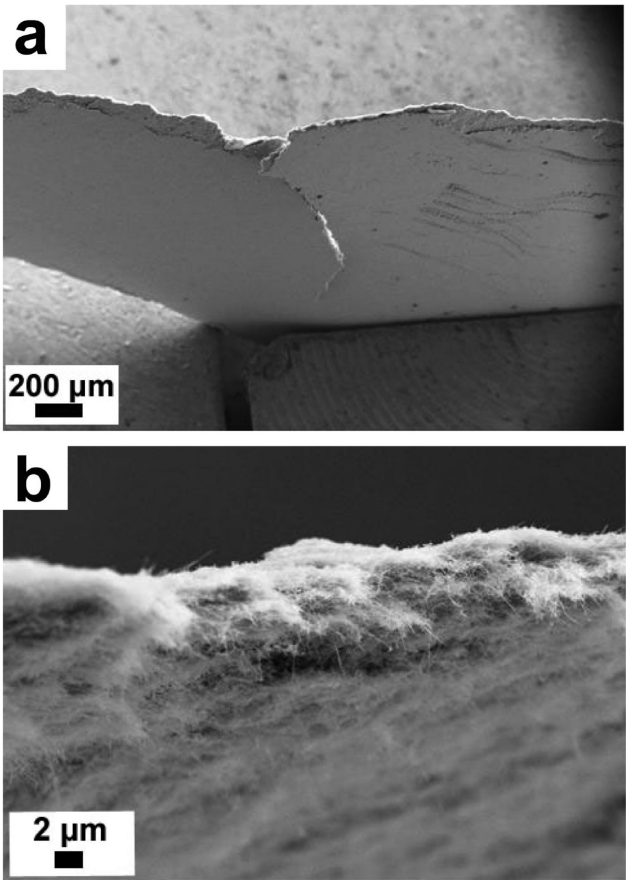

Figure 5. SEM images of $CuInSe_2$ nanowire fabric.

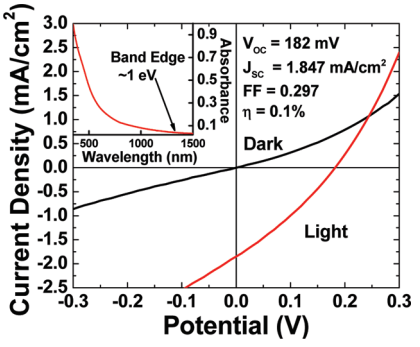

Figure 6. Current voltage characteristics of a CIS nanowire PV device. Inset: room-temperature UV−vis−near infrared (NIR) absorbance spectrum of CIS nanowires dispersed in toluene. The optical gap of approximately 1 eV corresponds to the bulk literature value of 0.95−1.05 eV for CIS.[26]

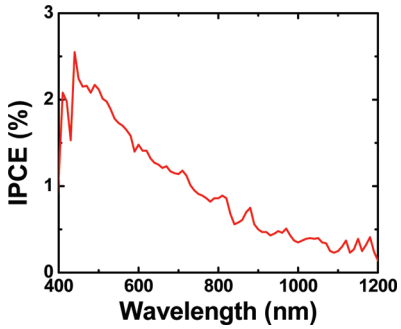

Figure 7. IPCE spectrum of a typical CIS nanowire PV device, measured at zero bias.

CONCLUSION

In summary, this is a first report of PV device fabrication incorporating solution-processed CIS nanowires. While the efficiency of these devices needs improvement, the absorber layer was not annealed or chemically treated in any way. Further synthetic improvements and optimization of the device fabrication should lead to PCE enhancement. There are also opportunities to combine nanowires with other materials, like nanocrystals or organics as well, to generate bulk heterojunction devices based on these nanowires. Another interesting concept is to create nonwoven fabrics from semiconductor nanowires,[28] which in this case of CIS might be used to create lightweight and flexible PV device structures to generate power from the sun.

ASSOCIATED CONTENT

Supporting Information. TEM images of Bi nanocrystals and the aggregated CIS reaction product obtained when Bi nanocrystals were not added to the reactions. This material is available free of charge via the Internet at http://pubs.acs.org.

AUTHOR INFORMATION

Corresponding Author
*E-mail: korgel@che.utexas.edu.

ACKNOWLEDGMENT

Financial support from the Robert A. Welch Foundation (Grant No. F-1464) and the Air Force Research Laboratory (FA8650-07-2-5061) is gratefully acknowledged. B.W.G. acknowledges financial support under the NSF IGERT Program DGE-054917. V.C.H. acknowledges the Fannie and John Hertz Foundation and the NSF Graduate Research Fellowship Program for financial support.

REFERENCES

(1) Repins, I.; Contreras, M. A.; Egaas, B.; DeHart, C.; Scharf, J.; Perkins, C. L.; To, B.; Noufi, R. *Prog. Photovoltaics Res. Appl.* **2008**, *16*, 235–239.
(2) Panthani, M. G.; Akhavan, V.; Goodfellow, B.; Schmidtke, J. P.; Dunn, L.; Dodabalapur, A.; Barbara, P. F.; Korgel, B. A. *J. Am. Chem. Soc.* **2008**, *130*, 16770–16777.
(3) Guo, Q.; Ford, G. M.; Hillhouse, H. W.; Agrawal, R. *Nano Lett.* **2009**, *9*, 3060–3065.
(4) Steinhagen, C.; Panthani, M. G.; Akhavan, V.; Goodfellow, B.; Koo, B.; Korgel, B. A. *J. Am. Chem. Soc.* **2009**, *131*, 12554–12555.
(5) Guo, Q.; Hillhouse, H. W.; Agrawal, R. *J. Am. Chem. Soc.* **2009**, *131*, 11672–11673.
(6) Gur, I.; Fromer, N. A.; Geier, M. L.; Alivisatos, A. P. *Science* **2005**, *310*, 462–465.
(7) Koleilat, G. I.; Levina, L.; Shukla, H.; Myrskog, S. H.; Hinds, S.; Pattantyus-Abraham, A. G.; Sargent, E. H. *ACS Nano* **2008**, *2*, 833–840.
(8) Choi, J. J.; Lim, Y.-F.; Santiago-Berrios, M. E. B.; Oh, M.; Hyun, B.-R.; Sun, L.; Bartnik, A. C.; Goedhart, A.; Malliaras, G. G.; Abruña, H. D.; Wise, F. W.; Hanrath, T. *Nano Lett.* **2009**, *9*, 3749–3755.
(9) Luther, J. M.; Law, M.; Beard, M. C.; Song, Q.; Reese, M. O.; Ellingson, R. J.; Nozik, A. J. *Nano Lett.* **2008**, *8*, 3488–3492.
(10) Hillhouse, H. W.; Beard, M. C. *Curr. Opin. Colloid Interface Sci.* **2009**, *14*, 245–259.
(11) Hochbaum, A. I.; Yang, P. *Chem. Rev.* **2009**, *110*, 527–546.
(12) Law, M.; Greene, L. E.; Johnson, J. C.; Saykally, R.; Yang, P. *Nat. Mater.* **2005**, *4*, 455–459.
(13) Huynh, W. U.; Dittmer, J. J.; Alivisatos, A. P. *Science* **2002**, *295*, 2425–2427.
(14) Yang, Y.-H.; Chen, Y.-T. *J. Phys. Chem. B* **2006**, *110*, 17370–17374.
(15) Phok, S.; Rajaputra, S.; Singh, V. P. *Nanotechnology* **2007**, *18*, 475601.
(16) Xu, J.; Lee, C.-S.; Tang, Y.-B.; Chen, X.; Chen, Z.-H.; Zhang, W.-J.; Lee, S.-T.; Zhang, W.; Yang, Z. *ACS Nano* **2010**, *4*, 1845–1850.
(17) Peng, H.; Schoen, D. T.; Meister, S.; Zhang, X. F.; Cui, Y. *J. Am. Chem. Soc.* **2006**, *129*, 34–35.
(18) Wooten, A. J.; Werder, D. J.; Williams, D. J.; Casson, J. L.; Hollingsworth, J. A. *J. Am. Chem. Soc.* **2009**, *131*, 16177–16188.
(19) Cowley, A. H. In *Inorganic Syntheses*; John Wiley & Sons: New York, NY, 1997; p 100.
(20) Davidson, F. M.; Lee, D. C.; Fanfair, D. D.; Korgel, B. A. *J. Phys. Chem. C* **2007**, *111*, 2929–2935.
(21) Norako, M. E.; Brutchey, R. L. *Chem. Mater.* **2010**, *22*, 1613–1615.
(22) Koo, B.; Patel, R. N.; Korgel, B. A. *Chem. Mater.* **2009**, *21*, 1962–1966.
(23) Spirkoska, D.; Arbiol, J.; Gustafsson, A.; Conesa-Boj, S.; Glas, F.; Zardo, I.; Heigoldt, M.; Gass, M. H.; Bleloch, A. L.; Estrade, S.; Kaniber, M.; Rossler, J.; Peiro, F.; Morante, J. R.; Abstreiter, G.; Samuelson, L.; Fontcuberta i Morral, A. *Phys. Rev. B* **2009**, *80*, 245325.
(24) Johansson, J.; Dick, K. A.; Caroff, P.; Messing, M. E.; Bolinsson, J.; Deppert, K.; Samuelson, L. *J. Phys. Chem. C* **2010**, *114*, 3837–3842.
(25) Fontcuberta i Morral, A.; Arbiol, J.; Prades, J. D.; Cirera, A.; Morante, J. R. *Adv. Mater.* **2007**, *19*, 1347–1351.
(26) Stanbery, B. J. *Crit. Rev. Solid State Mater. Sci.* **2002**, *27*, 73–117.
(27) Joyce, H. J.; Wong-Leung, J.; Gao, Q.; Tan, H. H.; Jagadish, C. *Nano Lett.* **2010**, *10*, 908–915.
(28) Smith, D. A.; Holmberg, V. C.; Korgel, B. A. *ACS Nano* **2010**, *4*, 2356–2362.